On the Effect of Component Mismatches in Inverter Interfaced Microgrids

Ramachandra Rao Kolluri, Tansu Alpcan
Iven Mareels and Marcus Brazil
Electrical and Electronic Engineering
The University of Melbourne

Julian de Hoog and Doreen Thomas
Department of Mechanical Engineering
The University of Melbourne

***Abstract*—In droop-controlled inverter-based microgrids, component mismatches and parameter drifts may have a significant effect on system stability. Analyzing this practical and important problem, it is shown that droop control is sensitive to such drifts and certain conditions have to be satisfied to maintain stability. Furthermore, these mismatches lead to a deviation in power sharing between the droop-controlled inverters even in the stable case. A central supervisory control that uses very low bandwidth communication is proposed to correct the resulting deviations. Simulation results of a simple microgrid example demonstrate the problem and the proposed solution.**

***Index*—Droop control, component mismatches, microgrid, inverter, sensitivity, power sharing error.**

I. Introduction

There has been an observable global shift towards renewable energy in order to reduce greenhouse gas emissions. The geographical clustering of these renewable energy sources together with improved energy storage technologies have paved the way for *microgrids* [1]. Microgrids are envisioned as an exciting opportunity for reducing carbon emissions. Combined together with other advantages such as uninterrupted supply of critical-loads (under grid interruptions) and reduced transmission (line) losses, efficient and reliable operation of microgrids has received much attention over the last decade. *Islanded* operation of microgrids with non-inertial generation connected via inverters is one of the main technical challenges addressed in the literature [1], [2].

Energy sources within the microgrid should be able to continue the microgrid operation in islanded mode i.e., regulate the voltage (V) and frequency (f) within permissible levels and maintain stability in the microgrid. Clearly the total energy available for dispatch is the limiting factor for microgrid operation in the islanded mode. It is therefore desirable to have a robust power sharing capability between sources in a microgrid, to enable maximal use of the available energy.

Power sharing between voltage source inverter (VSI) (hereinafter "inverter") based sources through *droop control* was originally proposed in [3]. Under droop control, each inverter in a microgrid measures its output real power (P) and reactive power (Q) and modifies the frequency (f) and voltage (V) to achieve proportional power sharing. Droop control is extensively discussed in [1], [4]–[7], including the dynamic and steady state stability of droop control, its applicability to various types of networks and accuracy in power sharing. The conventional frequency droop control methods involve $P-f$ and $Q-V$ droops. Depending on the network impedance these droops are modified into $P-V$ and $Q \pm f$ and known as *reversed* droop/boost control. Droop control can be considered as an imitation control where the inverters imitate synchronous generators to share power. The proportional power sharing and the availability of frequency (f) as a global variable are the advantages that follow such imitation control. Primary power sharing via *droop control* is distributed and no explicit communications are necessary [8].

In [9], the authors carried out a qualitative analysis to demonstrate the contribution of numerical errors, disturbances, noises, feeder impedance, parameter drifts and component mismatches to inaccuracy in power sharing[1]. A robust voltage controller was proposed to mitigate these effects. However, no efforts were made in describing the robustness of the network with respect to synchronization mismatches. Very few works [9]–[11] acknowledged the issues arising from frequency related mismatches but even so these are not exposed in great detail. In general, the research communities assume that the frequencies can be stable, which is not necessarily always the case.

The frequency output of an inverter is based on its internal clock. Even under normal operating conditions these inverters have a limited frequency setting/operating accuracy (represented in percentages of operating frequency). These bounds define the maximum and minimum frequency deviations the inverter system can experience. This behaviour of the inverters can cause parameter drifts in an interconnected scenario. Frequency mismatches can also occur from faulty inverters or unsynchronized "plug and play" interconnections. It is therefore important to include these tolerances into the microgrid design and stability criteria.

Contributions: This work explores how frequency mismatches in droop-controlled microgrids lead to instabilities. The contributions of this work are two-fold. Firstly, we introduce a frequency instability term into the dynamics of the

This work has been partly funded by a Linkage Grant supported by the Australian Research Council, Better Place Australia and Senergy Australia.

[1]Specifically those arising from voltage, $P-V$ droops were used for a low voltage network.

system. The effect of frequency mismatches arising from these instabilities is demonstrated. Subsequently, a relaxed condition for synchronization under frequency mismatches is presented. The condition holds for a specific network topology and under certain assumptions, which are discussed in detail. Secondly, it is shown that these mismatches can lead to a power sharing error (in steady state). Accurate power sharing is then restored using a central controller and communications.

Paper Organization: The remainder of the paper is organized as follows. The droop controlled system is described in Section II, where the component mismatch problem is formulated. Relaxed conditions for stability are presented in Section III, and a communication based power sharing error correction technique is proposed. The simulations and discussions are presented in Section IV, followed by conclusions and future work in Section V.

II. Problem Analysis

Power flow in AC Microgrids: An AC microgrid considered here is of a simple topology is considered as shown in Fig. 1. In general, the voltage magnitude of i^{th} bus is given by V_i and the phase angle θ_i. The phase angle between the i^{th} and the j^{th} bus is given by $(\theta_i - \theta_j) \in \mod(2\pi)$. To facilitate conventional droop control, we assume the networks are purely inductive ($Z_{ij} = Y_{ij}^{-1} = jX_{ij}$). In this case, the power flowing between buses is given by [12]

$$P_{ij} = V_i V_j |Y_{ij}| \sin(\theta_i - \theta_j) \tag{1}$$

Inverters and Droop Control: For this work, the distributed generation sources marked $i = \{1, 2....n\}$ in Fig. 1 output DC energy. This energy is converted into AC by individual inverters denoted by INV$_i$. The inverter output is filtered using a low pass LC filter (L_f, C_f) to reject the high switching frequency (f_{sw}) components and subsequently reduce the harmonic content of the output. All inverters are connected to a load bus through an output impedance (L_0) and supply a (lumped) load. The inverters can be modelled as voltage sources with defined values of output voltage and frequency [2]. It is assumed that the frequency changes are instantaneously reflected at the output.

In this scenario, the inverters use conventional droop control [3], [4] given in equation (2) to control their frequencies.

$$\omega_i = \omega^* - m_i(P_i^m - P_i^*) \tag{2}$$

$$\tau_{p_i} \dot{P_i^m} = -P_i^m + P_i \tag{3}$$

where m_i is the droop coefficient, ω_i is the instantaneous frequency, P_i^m is the measured instantaneous real power, ω^* and P_i^* are the reference frequency and real power set points, respectively. In practice, the measured power, P_i^m is filtered (to yield P_i) using a low pass filter (with time constant (τ_{p_i}), see equation (3)) to reduce the burden on the inverter controls. This makes the bandwidth of the voltage control loop much larger than the bandwidth of the droop controller. For this reason, the filter time constant τ_{p_i} has a strong effect on the dynamics (damping) of the system.

Kuramoto Oscillator Analogy: Another interesting perspective of microgrid operation was given in [13], [14] and references therein. The dynamics of the generalized "Kuramoto coupled oscillator" model obey

$$\dot{\theta_i} = \omega_i - \sum_{j=1}^{n} a_{ij} \sin(\theta_i - \theta_j), \qquad \forall i, j = \{1, 2....n\} \tag{4}$$

where θ_i is the angle between oscillator and an arbitrary reference and a_{ij} is the coupling strength between the oscillators i and j. On this basis, the droop controller (2) can be reformulated as

$$D_i \dot{\theta_i} = P_i^* - P_i \tag{5}$$

where $D_i = m_i^{-1}$, $\dot{\theta_i} = \omega^* - \omega_i$ and $P_i^m = P_i$ (i.e., disregarding the presence of the ripple filter, $\tau_{p_i} = 0$). Substituting P_i in (5) with that in (1) leads to

$$D_i \dot{\theta_i} = P_i^* - V_i V_0 |Y_{i0}| \sin(\theta_i - \theta_0) \tag{6}$$

For a constant power load P_0, all the power injections into the bus must be balanced (exactly equal to the the load).

$$P_0 = \sum_{i=1}^{n} V_i V_0 |Y_{i0}| \sin(\theta_i - \theta_0) \tag{7}$$

For maintaining mathematical consistency (with the Kuramoto model), a frequency dependent load term $D_0 \dot{\theta_0}$ is augmented to the load P_0 (however, it does not affect the system as $D_0 \to 0$). Subsequently, it was shown in [13] that the closed loop system can be represented as a network of coupled *multirate Kuramoto oscillators* with the rate constants D_i, natural frequencies P_i^* and the coupling strengths a_{i0} (can be defined as $a_{i0} \triangleq V_i V_0 |Y_{i0}|$). Such a system is said to be stable when the condition (8) (or equivalently, the condition (9)) is satisfied.

$$\Gamma := \max_{i \in \{1,....n\}} \left| \frac{P_i}{V_i V_0 |Y_{i0}|} \right| < 1 \tag{8}$$

(or)

$$\sin^{-1}(\Gamma) \equiv |\theta_i - \theta_0| \in [0, \frac{\pi}{2}) \tag{9}$$

We refer to [13] for derivation of equations (8) and (9), and associated proofs. Physically, the condition (8) means that the power flowing in the system should be less than the network physical limits given by $a_{i0} \triangleq V_i V_0 |Y_{i0}|$ to maintain stability [14]. The condition (9) is a well established phenomenon, which says, stability is achieved when the phase angle between any two buses is less than $\frac{\pi}{2}$ radians. Considering the thermal limits of the network, it is recommended to maintain $\max |\theta_i - \theta_0| \simeq 15^o$. The synchronization rate [13] proportional to $\cos(\sin^{-1}\Gamma)$ and the synchronization frequency ω_s, in steady state, is given in equation (10). On the other hand, the discussion made above assumes that the coupling strengths, a_{i0} are known and constant. This assumption is not valid when the inverters dynamically adjust their voltages to share Q (for example, under the action $Q - V$ droop control shown in equation (11)). The condition (8) still holds true if

the bus voltage magnitudes V_i and susceptances Y_{i0} are always maintained within their lower bounds ($\underline{V_i}$ and $\underline{Y_{i0}}$, respectively) as shown in equations (12) and (13) [13].

$$\omega_s = \frac{P_0 + \sum_{i=1}^{n} P_i^*}{\sum_{i=1\in} D_i} \tag{10}$$

$$V_i = V_i^* - k_i(Q_i^m - Q_i^*) \tag{11}$$

$$V_i > \underline{V_i} > 0 \tag{12}$$

$$|Y_{i0}| \geq |\underline{Y_{i0}}| > 0 \tag{13}$$

Generally, these bounds can be maintained if small droop coefficients (m_i and k_i) are chosen. Proper (proportional) power sharing in a droop controlled environment is achieved through the choice of m_i given by (14).

$$m_i P_i^* = m_j P_j^* \qquad \forall i, j = \{1, 2, \ldots n\} \tag{14}$$

Note that the coefficients m_i and k_i must, therefore, be selected with a knowledge of all the inverter ratings in the microgrid system.

Effect of frequency mismatches: Throughout the analysis, it was assumed that the frequency of each inverter is perfectly controllable and has a nominal value of $\omega_i^* = \omega_j^* = \omega^*$. As mentioned in Section I, the operating frequencies of inverters are not absolutely accurate or perfectly controllable. They will have a frequency setting accuracy and operating accuracy (both represented in percentages of their operating frequency). To understand the effect of these tolerances on the dynamics of the system, we can include all frequency mismatches in i^{th} inverter as an extra slow time-varying (bounded) frequency term, $\omega_{\epsilon,i}(t) \in \mathbb{R}$. The droop control law in equation (2) will subsequently change to

$$\omega_i(t) = \omega^* - m_i(P_i^m - P_i^*) + \omega_{\epsilon,i}(t) \tag{15}$$

Stability in the presence of these mismatches is currently not addressed in sufficient detail [9]–[11]. In the next section, we present some conditions that should hold to ensure stability of such a system. We define $\omega_{\epsilon,avg}(t) \triangleq \frac{1}{n}\sum_{i=1}^{n} \omega_{\epsilon,i}(t)$.

III. Conditions for Stability

In this work, we particularly focus on frequency stability of each inverter. While most work to date generally assumes that the inverters can maintain a particular frequency, in practice there can be fluctuations due to manufacturing flaws or clock inaccuracies. For example, 0.1% to 1% operating accuracy is considered to be a satisfactory design for commercial inverters. In the critical-load and energy-limited scenario, such as a microgrid, these small tolerances play a major role. It is advantageous to define the robustness of the system in terms of the "maximum deviation in frequency" for which the system can remain stable. Design engineers can make use of these conditions to design the microgrid and ensure stability and safe thermal limits. These conditions will ensure modularity or safer "plug and play" operation of inverters in a microgrid,

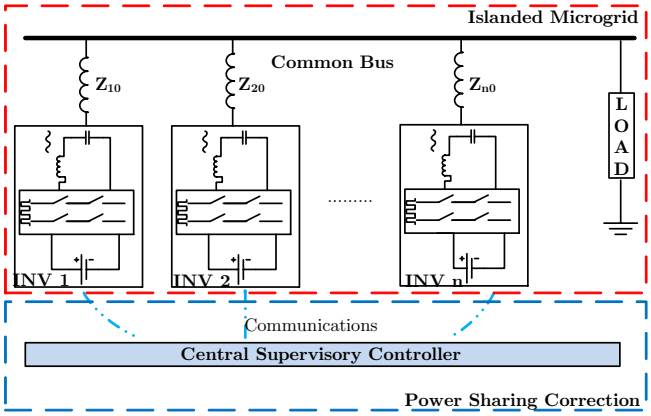

Fig. 1: (Red dashed region) Islanded microgrid set-up with n inverters connected to a common bus supplying a load. (Blue dashed region) Power sharing error correction using a central supervisory controller (CSC). Blue Dash-dot lines between inverters and CSC represent communication.

especially in those where the sources are operating very close to the stability margin (for example, in a highly stressed system with Γ in (8) approaches 1.)

From [13] and discussions made earlier, for a frequency droop controlled microgrid and under certain assumptions, the necessary and sufficient condition for synchronization is given in equation (8). To show how the frequency differences between inverters affect the stability of the system, we need to introduce the concept of power sharing error introduced by the term $\omega_{\epsilon,i}(t)$.

Theorem. ***Improved Stability Condition***

Consider a frequency droop controlled inverter system with operating frequency instabilities that are represented by $\omega_{\epsilon,i}(t)$. Then, system stability is ensured if

$$\Gamma_{new} = \max_{i=\{1,2\ldots n\}} \left|\frac{(P_i + D_i(\omega_{\epsilon,i}(t) - \omega_{\epsilon,avg}(t))}{\tilde{a_{i0}}}\right| < 1 \tag{16}$$

(or)

$$\sin^{-1}(\Gamma_{new}) \equiv |\theta_{i,new} - \theta_{0,new}| \in [0, \frac{\pi}{2}) \tag{17}$$

and the stable synchronized frequency is given by

$$\omega_{s,new}(t) = \frac{P_0 + \sum_{i=1}^{n} P_i^*}{\sum_{i=1}^{n} D_i} + \omega_{\epsilon,avg}(t) \tag{18}$$

Heuristic Argument If there exists a stable synchronization frequency $\omega_{s,new}$ even in the presence of a mismatch $\omega_{\epsilon,i}(t)$, then, the power sharing error (a similar result was presented in [9] for $Q + f$ boost) that will arise from this frequency difference is given by

$$P_{\epsilon,i}(t) = D_i(\omega_{\epsilon,i}(t) - \omega_{\epsilon,avg}(t)) \tag{19}$$

That means, the (new) physical limits of the system ($\tilde{a}_{i0}$)

must be larger than the power shift ($\max(P_i + D_i(\omega_{\epsilon,i}(t) - \omega_{\epsilon,avg}(t))$) introduced by the term $\omega_{\epsilon,i}(t)$, which is quite straightforward. Alternatively, this means that the microgrid will be able to achieve a frequency synchronization, $\omega_{s,new}$, when the frequency difference is small enough to limit the (new) phase angle between the buses to $< |\frac{\pi}{2}|$ radians. Since the synchronization rate depends on Γ_{new}, the smaller the frequency instabilities, the faster the system reaches a synchronized solution $\omega_{s,new}$. The value of $\omega_{s,new}$ is given by the frequency drop due to the total load ω_s together with the average frequency deviation due to all the uncertain frequencies ($\omega_{\epsilon,avg}(t) = \frac{1}{n}\sum_{i=1}^{n}\omega_{\epsilon,i}(t)$) in the microgrid. It is possible that the exact mismatches are not known, so the numerator in equation (16) can be modified as $\max(P_i + D_i(\omega_{\epsilon,max}(t) - \omega_{\epsilon,min}(t))$ to guarantee stability. The subscripts $min,\ max$ represent minimum and maximum frequency deviations. □

Therefore, for uncontrollable or fixed system parameters like total load $\sum P_i$ and output impedance $|Y_{i0}|$ we have control over the parameters m_i, k_i to satisfy equation (16). It remains to be shown, what effect the ripple filter time constant τ_{p_i} has on the dynamics of the system. It is shown in [15] that the system becomes underdamped with a large τ_{p_i} but the stability of the system is not directly affected by any valid choice of τ_{p_i}.

Although, the stability condition holds appropriately for constant power loads under the assumption of small droop coefficients, it is an overestimation in the case of constant impedance loads. This is due to the fact that, under constant impedance loads, the system is not fully decoupled and P_i is not $f(\theta)$ any more, instead $P_i = f(\theta, V)$. For example, a load increase causes a drop in the load voltage, reducing the amount of power consumed by the constant impedance. Choosing a small k_i for the design is important here because there is a compromise between the reduction in voltage and stability. As mentioned earlier, the increase in load will reduce the inverter and load voltage (voltage drop due to load increase + voltage drop due to the $Q - V$ droop [9]). This reduces the value $\tilde{a}_{i0}$ even further leading to a stressed network. It should also be noted that, even if the system is stable and a synchronized frequency is achieved, the power supplied will now be according to the proportional coefficients m_i together with the extra power as given by equation (19). Power sharing error correction is presented in section III-A.

A. *Power Sharing Correction*

As seen in the previous section, if the system is still stable with a $\omega_{\epsilon,i}(t)$, power sharing will be perturbed and reach a different value. Therefore, a supervisory control will be necessary to regulate the powers back to the desired values. In this work we propose a central supervisory controller (CSC, shown in Fig. 1) to facilitate this correction. The CSC receives power outputs of each inverter P_i periodically. The CSC then calculates the reference/desired power ($P_i^\dagger$) using

$$\frac{\sum_{i=1}^{n} P_i(t) \prod_{i=1}^{n} m_i}{m_i \sum_{j=1}^{n} \prod_{i=1}^{n} \left(\frac{m_i}{m_j}\right)} = P_i^\dagger(t). \tag{20}$$

It should be noted that this equation requires only the total load $\sum P_i$. Once the reference power is calculated, the new nominal power $P^*_{new,i}$ that should be supplied at each inverter is calculated according to

$$P^*_{new,i}(t) = P_i^\dagger(t) - P_i(t) \tag{21}$$

This information is then sent to each inverter, which ensures the desired power injection. This method will also be useful to eliminate the (smaller) power imbalances caused by various other mismatches such as, DC side characteristics and unsynchronized inverter addition etc. The communication bandwidth can be very low for the given example (for example, an update every 30 seconds) and hence the details will not be discussed. In the case of time varying $\omega_{\epsilon,i}(t)$, if the system is still stable according to condition (16), the variations can be corrected using this technique. Such a correction will require a communication bandwidth and triggering depending on the variance of $\omega_{\epsilon,i}(t)$.

IV. Simulations and Discussion

To illustrate our analysis, we simulated a simplified single-phase two inverter system ($n = 2$) with a simple load. The inverter system and control parameters are designed to achieve desired stability. Their parameters are given in Table I. The droop controllers were designed to power equally ($m_1 : m_2 = k_1 : k_2 = 1 : 1$). The voltage and power ratings were chosen to be low to facilitate potential experimental validation and the load is selected to be constant impedance, therefore, the results presented here are conservative.

A. *Ideal Case*

In this case, the frequencies of the INV_1 and INV_2 are set exactly to 50Hz, in other words, $\omega_{\epsilon,1} = \omega_{\epsilon,2} = 0$ Hz. The power sharing, in this case, is very similar to the results reported in the majority of the literature on inverter interfaced microgrids and shown in Fig. 2a. The simulation begins at time $t = 0$s and both inverters are switched ON. After sometime (depending on the time constant of the ripple filter τ_{p_i}, it is chosen to be 5 Hz in this example) each inverter supplies 122 W. At time $t = 10$s, an identical load is added in parallel and it can be seen that the real power injection of both the inverters increases to 195 W. The real power injected is not exactly double because the load is not true constant power load.

B. *Non-ideal Case*

The frequency of INV_2 is now increased by $\omega_{\epsilon,2} = 0.025$ Hz keeping the frequency of INV_1 constant at 50 Hz, i.e., $\omega_{\epsilon,1} = 0$Hz. As we can see from Fig. 2c and Fig. 2d, the microgrid reaches a synchronized frequency and stabilizes. The value of $|\theta_1 - \theta_2| = 0.9182$ radians $= 52.6^o < \frac{\pi}{2}$,

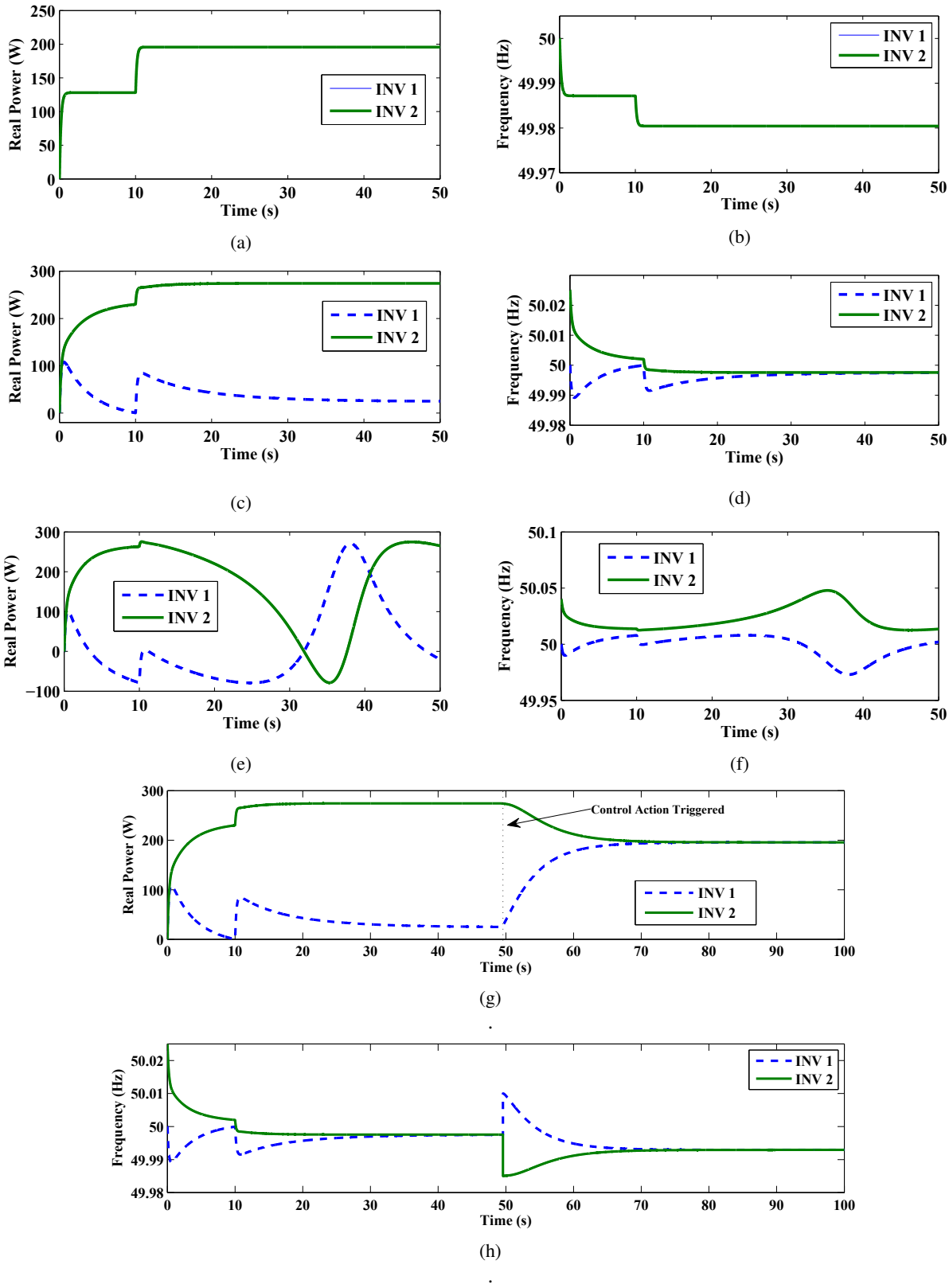

Fig. 2: Simulations Results of a two inverter system (INV_1 and INV_2) supplying a load. **Ideal Case** i.e., $\omega_{\epsilon,1} = \omega_{\epsilon,2} = 0$ Hz **(a)** Real Power outputs **(b)** Frequencies; **Non-Ideal Stable Case** i.e., $\omega_{\epsilon,1} = 0$ Hz and $\omega_{\epsilon,2} = 0.025$ Hz **(c)** Real Power outputs **(d)** Frequencies; **Non-Ideal Unstable Case** i.e., $\omega_{\epsilon,1} = 0$ Hz and $\omega_{\epsilon,2} = 0.04$ Hz **(e)** Real Power outputs **(f)** Frequencies; **Correction Technique** Triggered at around $t = 50$s **(g)** Real Power outputs **(d)** Frequencies. The angle between the inverters is reduced from $|\theta_1 - \theta_2| = 0.9182$ radians to $|\theta_1 - \theta_2| = 0$ radians by the triggered control action.

TABLE I: Simulation Parameters

Parameter	Value	Parameter	Value
f_{sw}	10 kHz	f_{cutoff}	800 Hz
V_{cp-p}	24 V	$L_f = L_0$	1.8 mH
C_f	22 μF	$V_{dc,OCV}$	40 V
$m_1 = m_2$	0.0001 Hz/W	$k_1 = k_2$	0.01 V/Var

thus ensuring stability. It is apparent from Fig. 2c that the output power of INV_2 is greater than that injected by INV_1 to compensate the frequency mismatch. It can be verified that the difference in the power is around 250 watts which is expected ($\because |\Delta P| = |P_2 - P_1| = 0.025/0.0001 = 250$Watts). However, when $\omega_{\epsilon,2} = 0.04$ Hz, the stability condition does not hold and the system goes unstable as shown[2] in Fig. 2e and Fig. 2f. The evolution of the angle between the inverters for all the cases is shown in Fig. 3.

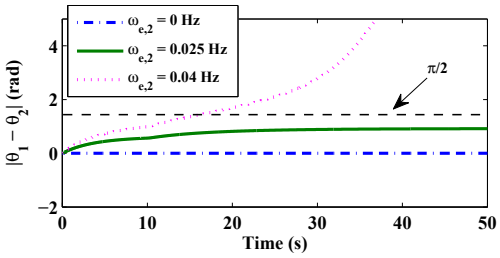

Fig. 3: Evolution of the angle between the inverters. Stability margin is marked as $\frac{\pi}{2}$ radians.

C. *Correction Technique*

In the case, when the INV_2 frequency is perturbed by $\omega_{\epsilon,2} = 0.025$ Hz, we have seen already that the system is stable and the power sharing is not according to their droop coefficients. In this section, we demonstrate the correction technique proposed in section III-A to correct the power sharing error. The global frequency $\omega_{s,new}$ does not accurately describe the load on the system. The central supervisory controller (CSC) receives the power information of both INV_1 and INV_2 periodically. The control action can be triggered manually or by set-point violation. For the purpose of demonstration, we use manual triggering of the control action at $t = 50$s. Once the control action is triggered, the CSC calculates the desired nominal power injections for each inverter using equation (20) and (21). The values are $P^*_{new,1} = 125$ W and $P^*_{new,2} = -125$ W. These values are sent to the INV_1 and INV_2 where the corrections will be made. Fig. 2g shows how the real power output injections are modified. It should be noted that the control action is independent of load changes and achieves proper error correction. For time varying errors the speed/mode of triggering and communication bandwidth have to be modified, accordingly.

[2]An implicit assumption is that the inverter is connected through a storage device which can inject or absorb power. Hence, the negative values of P refer to absorbed power.

V. Conclusion and Future Works

This work explored the impact of frequency mismatches on microgrid stability. A necessary and sufficient condition for the maximum mismatch in frequency that does not destabilize the system, under certain assumptions, was presented. Simulations were performed to show how the system stability is affected by the frequency mismatches. Following the stability discussion, a triggered control action based on a central controller and communications was proposed to correct the power sharing error. The corresponding simulation results show that the control action is effective and that the communication bandwidth required for the microgrid under consideration is very low. Verifying the effect of virtual impedance in achieving stability and exploring consensus based power correction algorithms are some possible research directions.

References

[1] R. Lasseter, "Microgrids," in *Power Engineering Society Winter Meeting, 2002. IEEE*, vol. 1, 2002, pp. 305–308 vol.1.

[2] J. Peas Lopes, C. Moreira, and A. Madureira, "Defining control strategies for microgrids islanded operation," *Power Systems, IEEE Transactions on*, vol. 21, no. 2, pp. 916–924, May 2006.

[3] M. Chandorkar, D. Divan, and R. Adapa, "Control of parallel connected inverters in standalone ac supply systems," *Industry Applications, IEEE Transactions on*, vol. 29, no. 1, pp. 136–143, Jan 1993.

[4] K. De Brabandere, B. Bolsens, J. Van den Keybus, A. Woyte, J. Driesen, and R. Belmans, "A voltage and frequency droop control method for parallel inverters," *Power Electronics, IEEE Transactions on*, vol. 22, no. 4, pp. 1107–1115, July 2007.

[5] J. Guerrero, J. Vasquez, J. Matas, L. de Vicua, and M. Castilla, "Hierarchical control of droop-controlled ac and dc microgrids x2014;a general approach toward standardization," *Industrial Electronics, IEEE Transactions on*, vol. 58, no. 1, pp. 158–172, Jan 2011.

[6] N. Pogaku, M. Prodanovic, and T. Green, "Modeling, analysis and testing of autonomous operation of an inverter-based microgrid," *Power Electronics, IEEE Transactions on*, vol. 22, no. 2, pp. 613–625, March 2007.

[7] J. Schiffer, R. Ortega, A. Astolfi, J. Raisch, and T. Sezi, "Conditions for stability of droop-controlled inverter-based microgrids," 2014, accepted for publication in Automatica.

[8] H. Liang, B. J. Choi, W. Zhuang, and X. Shen, "Stability enhancement of decentralized inverter control through wireless communications in microgrids," *Smart Grid, IEEE Transactions on*, vol. 4, no. 1, pp. 321–331, March 2013.

[9] Q.-C. Zhong, "Robust droop controller for accurate proportional load sharing among inverters operated in parallel," *Industrial Electronics, IEEE Transactions on*, vol. 60, no. 4, pp. 1281–1290, April 2013.

[10] T. Vandoorn, B. Renders, B. Meersman, L. Degroote, and L. Vandevelde, "Reactive power sharing in an islanded microgrid," in *Universities Power Engineering Conference (UPEC), 2010 45th International*, Aug 2010, pp. 1–6.

[11] A. Tuladhar, K. Jin, T. Unger, and K. Mauch, "Parallel operation of single phase inverter modules with no control interconnections," in *Applied Power Electronics Conference and Exposition, 1997. APEC '97 Conference Proceedings 1997., Twelfth Annual*, vol. 1, Feb 1997, pp. 94–100 vol.1.

[12] P. Kundur, N. Balu, and M. Lauby, *Power system stability and control*, ser. EPRI power system engineering series. McGraw-Hill, 1994.

[13] J. W. Simpson-Porco, F. Dorfler, and F. Bullo, "Synchronization and power sharing for droop-controlled inverters in islanded microgrids," *Automatica*, vol. 49, no. 9, pp. 2603 – 2611, 2013.

[14] J. Simpson-Porco, F. Dorfler, F. Bullo, Q. Shafiee, and J. Guerrero, "Stability, power sharing, amp; distributed secondary control in droop-controlled microgrids," in *Smart Grid Communications (SmartGridComm), 2013 IEEE International Conference on*, Oct 2013, pp. 672–677.

[15] E. Coelho, P. Cortizo, and P. Garcia, "Small-signal stability for parallel-connected inverters in stand-alone ac supply systems," *Industry Applications, IEEE Transactions on*, vol. 38, no. 2, pp. 533–542, Mar 2002.